

Softened Goldstone-Symmetry Breaking

Simone Blasi and Florian Goertz

*Max-Planck-Institut für Kernphysik
Saupfercheckweg 1, 69117 Heidelberg, Germany*

E-mail: simone.blasi@mpi-hd.mpg.de, fgoertz@mpi-hd.mpg.de

ABSTRACT: We propose a new way of breaking the Goldstone symmetry in composite Higgs models, restoring the global symmetry in the mixings between the elementary and composite fermions by completing the former to full representations of this symmetry. The Goldstone symmetry is in turn broken softly by vector-like mass terms in the *elementary* sector only. The resulting softened explicit breaking allows for a light Higgs boson, as found at the LHC, and a heavy top quark, without the need of light top partners around the Goldstone scale $f \sim \text{TeV} \ll m_{\text{comp.}}$, which remain elusive at the LHC, while we recover the standard scenario in the limit of infinite vector-like masses.

Contents

1	Introduction	1
2	General Setup	2
3	Explicit Results in Two-Site Model	4
3.1	Hierarchies in the elementary sector	6
3.2	No hierarchies in the elementary sector	9
4	Benchmark points	11
5	The general case of vector-like elementary fermions	12
6	Conclusions	13

1 Introduction

Composite Higgs (CH) models offer a promising means to solve the hierarchy problem since the Higgs boson is no longer a fundamental scalar but rather a bound state of a new strong interaction, that can be resolved above the TeV scale, and its mass is thus saturated in the IR [1–3]. Moreover, the conventional assumption of the Higgs being a (pseudo-)Goldstone boson of a spontaneously broken global symmetry ($SO(5) \rightarrow SO(4)$ in minimal models) provides a reasoning for its lightness compared to other new states. In the same framework, partially composite fermions (elementary fields mixing linearly with the composite sector of bound states) can also explain the hierarchical structure of fermion masses and mixings [4–7] and provide a dynamical origin for EWSB, mostly triggered by the large top-quark compositeness. The latter explicitly breaks the global symmetry, since the Standard Model (SM) fermions do not fill complete representations of the global symmetry that could couple to the composite sector in an invariant way, and thereby induces a potential for the Goldstone Higgs, intertwining flavor and EWSB.

Minimal models are however already in tension with the absence of *light top partners* at the LHC, which are required to keep the Higgs light by reducing the Goldstone-symmetry breaking [7–11], threatening the viability of explicit CH incarnations (see, e.g., [12]). While one possibility to avoid this is the inclusion of a realistic lepton sector generating small neutrino masses, which can have a larger impact on the Higgs potential than naively expected [13] with interesting consequences

for flavor physics [12–16]¹, here we want to explore an orthogonal solution, changing in fact the nature of the explicit Goldstone symmetry breaking.

Indeed, the latter could be significantly reduced if the SM fermions would be uplifted to complete representations of the global symmetry. In that case, their mixing with the composite sector, determining their degree of ‘compositeness’, would no longer violate the global symmetry. Since we did not observe additional light fermions so far, the symmetry still needs to be broken, which can however now be done by introducing vector-like mass terms for the new *elementary* fermions. This will shift the source of explicit breaking to a different sector and thereby corresponds to a fundamentally different approach of breaking the Goldstone symmetry. The breaking is now ‘soft’, since induced by mass terms in the elementary sector. Contrary to the conventional case, the underlying interactions between the SM fermions and the constituents of the composite states are now symmetry preserving. In particular, the setup will lead to a different parameteric structure of the mass of the composite Higgs, with the potential to lift the light top partners. The purpose of this article is to work out the phenomenological and conceptual consequences of this approach. Here, we focus on the minimal $SO(5)/SO(4)$ composite Higgs scenario [5], but the considerations can easily be extended to different cosets.

This article is organized as follows. In Sec. 2, we will introduce the setup, including the field content and corresponding $SO(5)$ representations, and will discuss the nature of breaking of the Goldstone symmetry. In Sec. 3 we will confront our general discussion with explicit results obtained for a two-site incarnation of the CH framework. After that, in Sec. 4, we will present benchmark spectra for our scenario of soft (vector-like) Goldstone breaking (sGB), while in Sec. 5 we demonstrate that raising the top partners is really related to a symmetry and not accidental. Finally, we conclude in Sec. 6.

2 General Setup

We consider just the third generation of quarks and lift the elementary fields to complete $SO(5)$ multiplets, mixing linearly with the composite resonances $\tilde{\Psi}^T = U(Q, \tilde{T})^T$, which have been decomposed into fourplets and singlets under the unbroken $SO(4)$ subgroup via the CCWZ prescription, with U the Goldstone matrix. The mixings with the resonances now respect $SO(5)$, and its explicit breaking is sequestered to the elementary sector.²

¹See also [17] for a solution via an enlarged quark sector.

²Note that the impact of the multiplets corresponding to the lighter generations on the Higgs potential remains negligible due to their small degree of compositeness. Moreover, the corresponding elementary vector-like partners can lie much above the compositeness scale, effectively recovering the conventional case.

We recall that in the MCHM₅ [7], the left-handed doublet q_L and the singlet t_R are embedded as

$$\psi_L^t = \Delta_L^{t\dagger} q_L \sim \mathbf{5}_{2/3}, \quad \psi_R^t = \Delta_R^{t\dagger} t_R \sim \mathbf{5}_{2/3}, \quad (2.1)$$

where the spurions

$$\Delta_L^t = \frac{1}{\sqrt{2}} \begin{pmatrix} 0 & 0 & 1 & -i & 0 \\ 1 & i & 0 & 0 & 0 \end{pmatrix}, \quad \Delta_R^t = -i \begin{pmatrix} 0 & 0 & 0 & 0 & 1 \end{pmatrix} \quad (2.2)$$

parameterize the $SO(5)$ breaking due to the fact that they do not fill complete $SO(5)$ multiplets. In the proposed vector-like extension with soft Goldstone breaking, the sMCHM₅, we augment ψ_L^t and ψ_R^t to full $SO(5)$ representations by introducing two (vector-like) elementary $SU(2)_L$ doublets, w and v , and a singlet, s , such that

$$\psi_L^t = \Delta_L^{t\dagger} q_L + \Delta_w^\dagger w_L + \Delta_s^\dagger s_L, \quad \psi_R^t = \Delta_R^{t\dagger} t_R + \Delta_w^\dagger w_R + \Delta_v^\dagger v_R, \quad (2.3)$$

where

$$\Delta_s = \Delta_R^t, \quad \Delta_v = \Delta_L^t, \quad \Delta_w = \frac{1}{\sqrt{2}} \begin{pmatrix} 1 & -i & 0 & 0 & 0 \\ 0 & 0 & 1 & i & 0 \end{pmatrix}. \quad (2.4)$$

The mass Lagrangian in the elementary sector reads

$$-\mathcal{L}_{\text{el}} = m_w(\bar{w}_L w_R + \bar{w}_R w_L) + m_v(\bar{v}_L v_R + \bar{v}_R v_L) + m_s(\bar{s}_L s_R + \bar{s}_R s_L) \\ + (m_1 \bar{s}_L t_R + m_2 \bar{q}_L v_R + \text{h.c.}), \quad (2.5)$$

allowing to make the new fermions heavy via vector-like mass terms, and can be rewritten in terms of the conventional $\Delta_{L,R}^t$ spurions as

$$-\mathcal{L}_{\text{el}} = m_w \bar{\psi}_L^t \psi_R^t + m_v \bar{v}_L \Delta_L^t \psi_R^t + m_s \bar{s}_R \Delta_R^t \psi_L^t + \\ \{ (m_2 - m_w) \bar{q}_L \Delta_L^t \psi_R^t + (m_w + m_1) \bar{\psi}_L^t \Delta_R^{t*} t_R + \text{h.c.} \}. \quad (2.6)$$

The elementary fields ψ_L^t and ψ_R^t formally mix with the composite resonances as in the MCHM₅, i.e. (see e.g. [7, 18]),

$$\mathcal{L}_{\text{mass}} = -m_Q \bar{Q}_L Q_R - \tilde{m}_T \bar{\tilde{T}}_L \tilde{T}_R \\ - y_L f \bar{\psi}_{LI}^t \left(a_L U_{Li} Q_R^i + b_L U_{I5} \tilde{T}_R \right) \\ - y_R f \bar{\psi}_{RI}^t \left(a_R U_{Li} Q_L^i + b_R U_{I5} \tilde{T}_L \right) + \text{h.c.}, \quad (2.7)$$

where only the lightest top partners are kept and f is the Goldstone-Higgs decay constant. As mentioned, this mixing does not break explicitly $SO(5)$, while new sources of $SO(5)$ breaking emerge in the elementary sector via the vector-like masses (2.5).

We note that in the 5D holographic dual (see [5–7]), our setup would correspond to choosing the same boundary conditions for *all* components of the fermionic bulk

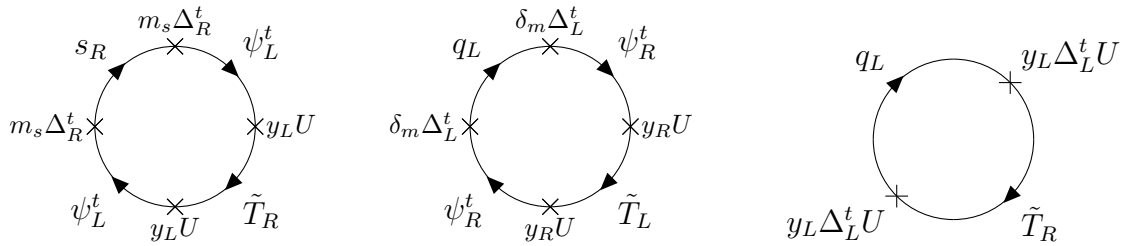


Figure 1. Two possible contributions to the Higgs potential in the sMCHM₅ (left), where $\delta_m \equiv m_2 - m_w$, compared to the MCHM₅ (right).

fiveplets of $SO(5)$ – whose zero-modes contain the SM fermions – thereby respecting $SO(5)$ at the first place. The additional zero-modes that emerge due to these universal boundary conditions are then projected out via finite ($SO(5)$ breaking) vector-like boundary mass terms on the UV brane, instead of employing dedicated boundary conditions to remove them (as in the conventional approach), which would correspond to the limit of infinite vector-like masses. This is similar to realizing EWSB via coupling to an IR-localized Higgs sector with a finite vev, instead of employing dirichlet boundary conditions to remove the massless modes of the weak gauge fields.

The different $SO(5)$ breaking results in a modified spurion structure for the Higgs potential. In the MCHM₅, the spurions were given by the linear mixings $y_{L,R} \Delta_{L,R}^t$, which always come together with the Goldstone matrix U . In the sMCHM₅, however, the $SO(5)$ breaking is given by the vector-like masses in the elementary sector, and thus an extra interaction is needed to make the Goldstone matrix enter the loop. This is schematically shown in Fig. 1 for two example contributions, corresponding to the third and fourth term in Eq. (2.6). In the next section, we will turn to a quantitative analysis of the Higgs potential – focusing on the interplay of the Higgs mass and the top-partner masses – where we will in particular see that the latter can be considerably lifted in the sGB setup, while in the limit of heavy vector-like masses the sMCHM₅ recovers the properties of the MCHM₅.

3 Explicit Results in Two-Site Model

We perform our quantitative analysis in a two-site implementation of the sGB scenario, where only the first layer of resonances is kept in the spirit of discrete models, see [11, 18]. Such a setup has the major advantage of being simple and transparent, but does not give a fully calculable Higgs potential, which is however not required for our study. The two-site model is given explicitly by the Lagrangian (2.7), with $a_L = a_R = b_L = b_R = 1$, together with the elementary fields, whose dynamics is specified by (2.6).

The Coleman-Weinberg potential for the Higgs field is given by

$$V(h) = -\frac{2N_c}{8\pi^2} \int_0^\infty dp p^3 \ln \{ \det[p^2 \mathbf{1} + m^\dagger m(h)] \}, \quad (3.1)$$

where $m(h)$ is the field-dependent fermion mass matrix, such that

$$\det[p^2 \mathbf{1} + m^\dagger m(h)] = 1 + a(p^2) \sin^2(h/f) + b(p^2) \sin^4(h/f), \quad (3.2)$$

where $a(p^2)$ and $b(p^2)$ are functions of the fermion masses. Expanding the logarithm up to $\sin^4(h/f)$, one finds

$$V(h) = \alpha \sin^2(h/f) + \beta \sin^4(h/f), \quad (3.3)$$

leading to the Higgs mass

$$m_h^2 = 2\beta/f^2 \sin^2(2v/f), \quad (3.4)$$

where

$$\alpha = -\frac{2N_c}{8\pi^2} \int dp p^3 a(p^2), \quad \beta = -\frac{2N_c}{8\pi^2} \int dp p^3 \left(b(p^2) - \frac{a^2(p)}{2} \right). \quad (3.5)$$

We find that α diverges logarithmically and β is finite at the order $\mathcal{O}(y_{L,R}^4)$, as in the two-site MCHM₅. The divergence of α can be cured introducing a renormalization scale μ , which is fixed to reproduce the correct Higgs vacuum expectation value (vev). As a consequence, $v \lesssim f$ does not require $a(p^2) \lesssim b(p^2)$, so that $a^2(p^2)$ and $b(p^2)$ can, a priori, equally contribute to β . Notice that, despite the divergence in α , the relation between the Higgs mass and the fermion masses is still predictable in the two-site model in terms of β .

In the MCHM₅, the top quark mixes with the doublet within Q sharing the quantum numbers of q_L , denoted by T , and with \tilde{T} , the singlet with t_R quantum numbers. In the sMCHM₅, there are two corresponding doublets, identified with the two superpositions of Q and the elementary doublet v , which we denote by T_+ and T_- . Similarly, \tilde{T} splits into two states, made out of \tilde{T} and s and referred to as \tilde{T}_+ and \tilde{T}_- . As a consequence, the expression for the top mass is modified in the sMCHM₅, reading

$$m_t^2 = y_L^2 y_R^2 f^4 \frac{m_s^2 m_v^2 (m_Q - \tilde{m}_T)^2}{8m_{T_+}^2 m_{T_-}^2 m_{\tilde{T}_+}^2 m_{\tilde{T}_-}^2} \sin^2(2v/f). \quad (3.6)$$

In the limit of large m_s and m_v , one can check that the elementary fields effectively decouple and Eq. (3.6) approaches the result of the MCHM₅ [8], i.e.

$$m_t^2 = y_L^2 y_R^2 f^4 \frac{(m_Q - \tilde{m}_T)^2}{8m_T^2 m_{\tilde{T}}^2} \sin^2(2v/f). \quad (3.7)$$

Since the vector-like masses for the different elementary fermion species, s, v , and w , are in general independent quantities, we divide our analysis in two parts. In Sec. 3.1 we assume that only one vector-like fermion is active below the cutoff scale $4\pi f \simeq 10 \text{ TeV}$ for $\xi = v^2/f^2 = 0.1$, while the other two are much heavier. The case in which all the elementary states are active, on the other hand, is presented in Sec. 3.2.

3.1 Hierarchies in the elementary sector

We start considering the case in which the singlet s is much lighter than v and w . The top mass is then given by

$$m_t^2 = y_L^2 y_R^2 f^4 \frac{m_s^2 (m_Q - \tilde{m}_T)^2}{8m_T^2 [m_{\tilde{T}}^2 m_s^2 + (y_L y_R f^2 + m_1 \tilde{m}_T)^2]} \sin^2(2v/f), \quad (3.8)$$

where $m_T^2 = m_Q^2 + y_L^2 f^2$, $m_{\tilde{T}}^2 = \tilde{m}_T^2 + y_R^2 f^2$. From (3.8), we see that the value for m_t in the sMCHM₅ is always smaller than in the MCHM₅, which can be recovered for $m_s \rightarrow \infty$. By itself, this effect would drive the top partners to be even lighter than in the MCHM₅. However, this is changed when the modification in the Higgs potential is taken into account.

In the following, we focus on β , which is calculable in the two-site model and determines the Higgs mass (3.4). For simplicity, we consider from now on the case in which the mixing between the chiral and the vector-like elementary fermions is negligible, namely $m_{1,2} = 0$ in (2.5). By looking at (3.5), one can see that the $a^2(p^2)$ term always increases the value of β . Its effect was found to be (accidentally) small for the two-site MCHM₅ in [8]. In the two-site sMCHM₅, it can instead be sizeable when all the vector-like fermions are light. However, if only one of them happens to be active below the cut-off, as discussed in this section, the $a^2(p^2)$ term can be safely neglected. Within this approximation, we find

$$\beta \simeq y_L^2 y_R^2 f^4 (m_Q - \tilde{m}_T)^2 \int_0^\infty dp p^3 \frac{(p^2 + \tilde{m}_T^2) m_s^2 - p^2 (p^2 + m_T^2)}{2p^2 (p^2 + m_{\tilde{T}_+}^2) (p^2 + m_{\tilde{T}_-}^2) (p^2 + m_T^2) (p^2 + \tilde{m}_T^2)}. \quad (3.9)$$

Notice that, compared to the two-site MCHM₅, there is one more propagator associated with the splitting of \tilde{T} to \tilde{T}_\pm .

In the limit of $y_{L,R} f$ much smaller than the mass of the vector-like fermions, we approximate the top mass as

$$m_t^2 \simeq \frac{y_L^2 y_R^2 f^4}{8m_Q^2} (q-1)^2 \sin^2(2v/f), \quad (3.10)$$

while β reads

$$\beta(r^2) \simeq \frac{N_c}{16\pi^2} y_L^2 y_R^2 f^4 \frac{(1-q)^2}{1-q^2 r^2} [(r^2 + 1/q^2) F(q^2) - 2F(r^2)], \quad (3.11)$$

where $q = m_Q/\tilde{m}_T$, $r = \tilde{m}_T/m_s$, and $F(x^2) = \frac{x^2}{1-x^2} \ln \frac{1}{x^2}$. One can show that

$$\beta(r^2) - \beta(0) = -\frac{N_c}{16\pi^2} y_L^2 y_R^2 f^4 (1-q)^2 \frac{F(q^2) - F(1/r^2)}{q^2 - 1/r^2} \leq 0, \quad (3.12)$$

where we have used $F(1/x^2) = F(x^2)/x^2$ and $F'(x) > 0$ for $x > 0$. The $\beta(0)$ term in (3.12) corresponds to the case in which the new singlet s is infinitely heavy and decouples. We checked that it coincides with the conventional formula for β in the two-site MCHM₅, namely

$$\beta(0) \simeq \frac{N_c}{16\pi^2} y_L^2 y_R^2 f^4 \frac{(1-q)^2}{q^2} F(q^2). \quad (3.13)$$

As expected, Eq. (3.12) shows that including the singlet s always reduces the amount of Goldstone breaking, leading to a lighter Higgs boson. Combining (3.10) and (3.11), we find

$$m_Q^2 = \frac{1}{16} y_L^2 y_R^2 f^2 \frac{(1-q)^2}{\beta(r^2)} \left(\frac{m_h}{m_t} \right)^2, \quad (3.14)$$

which relates the Higgs mass to the spectrum of resonances. By inspecting (3.11), we see that $\beta(r^2)$ vanishes for $q^2 r^4 = 1$ and it becomes negative for $q^2 r^4 > 1$, the latter being in conflict with a viable electroweak symmetry breaking. Approaching $q^2 r^4 = 1$, all the fermions besides the top can be arbitrarily heavy while still keeping the Higgs light. However, such an extreme configuration corresponds to infinite tuning in the parameter space and thus it is never realized in a realistic scan, as we will see below, where the effects remain finite. Nevertheless, this qualitative behavior shows an important feature of the sGB. In the MCHM₅, β can be small only for $q \rightarrow 1$, namely when $SO(5)_R$ is restored. This implies that the top mass would vanish in the same limit, thus making this region disfavored. In the sGB scenario, on the other hand, the breaking of the Goldstone symmetry is reduced by the new degrees of freedom, see (3.12). This effect does not interfere much with the top mass, Eq. (3.10) being indeed independent of r to first approximation. Therefore, the Higgs potential and the top mass can be disentangled such that a small β does not necessarily imply a light top (which could be lifted only via ultra-light partners).

As an estimate for the mass of the lightest eigenstate of the system, m_l , we take

$$m_l^2 \simeq \min\{m_Q^2, \tilde{m}_T^2, m_s^2\} = m_Q^2 \times \min\left\{1, \frac{1}{q^2}, \frac{1}{q^2 r^2}\right\} = m_Q^2 \times \min\left\{1, \frac{1}{q^2}\right\} \quad (3.15)$$

where m_Q^2 is given in (3.14). The estimate above is correct up to mixing terms $\sim y_{L,R} f$. The last equality in (3.15) is derived as follows. By definition, m_s can be the lightest state only for $r^2 \geq 1$ and $r^2 \geq 1/q^2$. Moreover, r and q must satisfy $r^2 \leq r_0^2 = 1/|q|$, as discussed below (3.14). However, if $|q| > 1$ one immediately derives the contradiction $r^2 < 1$, while if $|q| < 1$ one has $r^2 \geq 1/q^2 = r_0^4 > r_0^2$, which is clearly not compatible with $r^2 \leq r_0^2$. In conclusion, the spectrum favors a

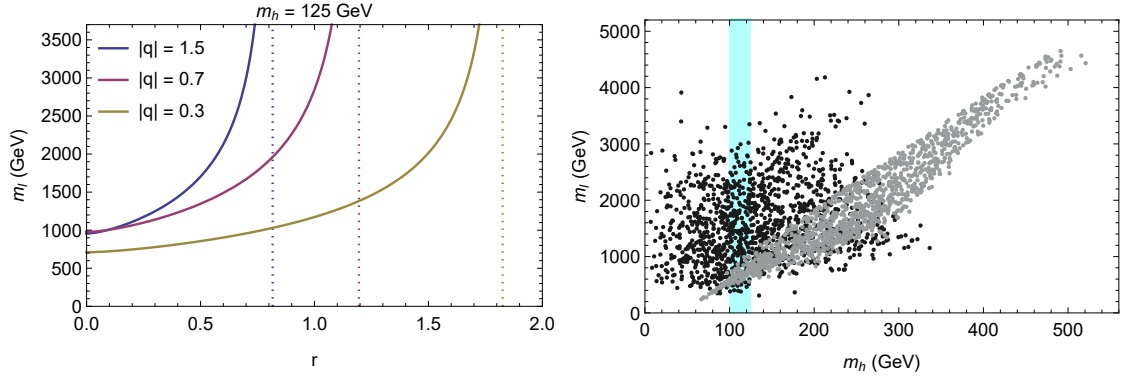


Figure 2. Left: The mass of the lightest top partner for different values of $|q|$ as a function of $r = \tilde{m}_T/m_s$ for $m_h = 125$ GeV. The dashed vertical lines indicate the value of r for which $q^2 r^4 = 1$. The result is the same for $r \rightarrow -r$. **Right:** Scatter plot of (m_h, m_l) for $0.5 \leq |r| \leq 2$ (black points) and $r = 0$ (gray points). We scan in the range $0.5 \leq |y_{L,R}| \leq 2$ and $0.5 \leq |\tilde{m}_T/\text{TeV}| \leq 4.5$ such that $-2 \leq q \leq -0.3$.

configuration with the elementary singlet s not residing at the bottom. When the latter is about to become the lightest state, β flips sign and the electroweak vacuum is no longer a minimum.

The value of m_l , as predicted by (3.15), is shown in the left panel of Fig. 2 as a function of r for different values of q . We take $m_t \simeq 150$ GeV for the top mass at the scale f . The result of the MCHM₅ is recovered for $r = 0$. The mass of the lightest state always increases with r until it hits the bound $q^2 r^4 = 1$, shown by the dotted vertical lines. It is important to notice that m_l can be significantly heavier than in the standard case for values of r and q which are far from $q^2 r^4 = 1$. Thus, a heavier m_l does not correspond to fine tuning in the parameter space but rather to a general prediction of the sMCHM₅. This is confirmed by the results shown in the right panel of Fig. 2, where (m_h, m_l) are obtained as an output from a numerical scan, using the exact expression for β (including the $a^2(p^2)$ term in (3.5)). The window $100 \text{ GeV} \leq m_h \leq 125 \text{ GeV}$, visualized by the blue stripe, is considered to take into account running effects on the actual value of the Higgs mass at the scale f . The mass ratio r is scanned between $0.5 \leq |r| \leq 2$ (black points). Gray points correspond to the MCHM₅, i.e. $r = 0$. The effect of the singlet s can be seen as effectively reducing the Higgs mass which is consistent with a certain value of m_l . For instance, $m_l \simeq 3$ TeV is compatible with $m_h \approx 100$ GeV in the sMCHM₅, whereas that would require $m_h \gtrsim 300$ GeV in the conventional case. This is just an equivalent way of looking at (3.12), where the ratio $\beta(r^2)/\beta(0) = m_h^2(r^2)/m_h^2(0) < 1$ gives the correct estimate for the compression of the Higgs spectrum.

Turning to the other cases, the situation in which only one of the doublets is light, either w or v , corresponds to a much more modest change with respect to the MCHM₅. In both cases, the $a^2(p^2)$ term in (3.5) is found to be small. The expression

for β driven by w in isolation matches the conventional result at the order $\mathcal{O}(y_{L,R}^4)$. On the other hand, v does reduce β at the $\mathcal{O}(y_{L,R}^4)$, its effect being however more modest due to an accidental factor $1/2$ in front of $F(r^2)$ (to be compared with a factor of 2 in (3.11)):

$$\beta(r^2) \simeq \frac{N_c}{16\pi^2} y_L^2 y_R^2 f^4 \frac{(1-q)^2}{1-q^2 r^2} [(1/q^2 - r^2/2)F(q^2) - F(r^2)/2], \quad (3.16)$$

where $q = m_Q/\tilde{m}_T$, as before, while now $r = \tilde{m}_T/m_v$. The fact that the contribution of the doublets is modest in isolation does not mean that they are always negligible. In particular, the Goldstone symmetry can be in principle restored only if all the elementary vector-like states are active. Of course, too light states are in conflict with the LHC searches, the intermediate region being the topic of the next section.

3.2 No hierarchies in the elementary sector

We finally discuss the results for the case in which no hierarchies are introduced among the elementary vector-like fermions s , v and w . To this end, we derived an expression for β following the same procedure that lead to (3.11), setting $m_v = m_w \equiv m_d$ for simplicity, which we refer to as β_f in the following. The relative spread between the elementary states is parameterized by $x = m_d/m_s$, while $r = \tilde{m}_T/m_s$ relates the elementary state s to the composites. We notice that the $a^2(p^2)$ term in (3.5) can actually be important for $x = \mathcal{O}(1)$. The lightest state m_l is now estimated as

$$m_l^2 \simeq \min\{m_Q^2, \tilde{m}_T^2, m_s^2, m_d^2\} = m_Q^2 \times \min\left\{1, \frac{1}{q^2}, \frac{1}{q^2 r^2}, \frac{x^2}{q^2 r^2}\right\}, \quad (3.17)$$

while the top mass is still approximated by (3.10). The quantity m_Q obeys (3.14), where β is now replaced by β_f .

We have checked that β_f approaches zero for $r \rightarrow \infty$, corresponding to massless elementary fermions and thus restoring the Goldstone symmetry. In practice, such limit is not of much use because it would introduce very light states in the spectrum. Nevertheless, while approaching this limit, β_f can have a zero also at an intermediate value of r depending on x and q . Although this is never realized in a realistic scan, the possibility of getting close to it without affecting the top mass again shows the new feature of the sGB.

We identify three different regions depending on the structure in the elementary sector, i.e., on the value of x . For $|x| \leq 2$, the improvement in the sMCHM₅ is modest and m_l can be roughly 2 TeV at most. The case of a large $|x|$ actually corresponds to the singlet case discussed at the beginning of Sec. 3.1. Thus, we here focus on the intermediate case $2 \leq |x| \leq 4$.

The analytical prediction based on β_f is shown in the left panel of Fig. 3 for $x = 2.7$. The knees signal that the elementary singlet becomes the lightest state. This happens for r such that $r^2 \geq r_q^2 = \max(1, 1/q^2)$. Notice that this was not

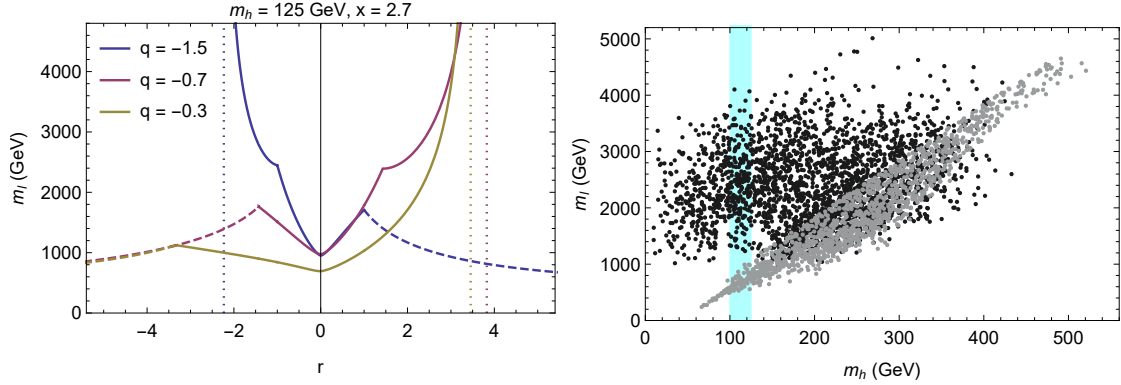


Figure 3. **Left:** Analytical approximation for the mass of the lightest top partner in the case $m_w = m_v = m_d$ for $q = (-1.5, -0.7, -0.3)$ as a function of $r = \tilde{m}_T/m_s$ with $m_h = 125$ GeV and $x = m_d/m_s = 2.7$. The vertical dotted lines indicate r such that $\beta_f = 0$ for the different values of q . The dashed curves show configurations for which the decrease in m_l is driven by the lightness of the new singlet. **Right:** The mass of the lightest top partner, m_l , as a function of m_h in the sMCHM₅ (black points) and in the MCHM₅ (gray points). The scan for the sMCHM₅ assumes $1 \leq |y_{L,R}| \leq 2$ and $-2 \leq q \leq -0.3$. Moreover, we consider $5 \text{ TeV} \leq |\tilde{m}_T| \leq 10 \text{ TeV}$, while $1.5 \leq |r| \leq 5$. The doublet masses $m_{w,v}$ are scanned independently in the range $2 \leq |m_{w,v}/m_s| \leq 4$. The scan for the MCHM₅ is the same as in Fig. 2. All the mass eigenstates reside below 15 TeV.

possible in the case in which the w and v doublets are infinitely heavy, since it would give a negative value of β , as discussion below (3.15). The dotted lines show the location of r such that β_f formally vanishes. The values of r above the dotted lines actually lead to a viable m_l , its value being just too large to be shown in the plot. Although such high masses are cut-off in a realistic scenario, this shows that the range of r leading to a viable electroweak symmetry breaking is enlarged with respect to the singlet case (see, e.g, the left panel of Fig. 2).

Since the largest m_l is typically found above the knee, a heavy top partner favors the case of the singlet s as the lightest particle. This implies that the spectrum can be stabilized without requiring the spin-1/2 resonances to lie much below the naive cutoff of the strong dynamics, as needed in the conventional case to reproduce the correct Higgs mass.

We explore this region of the parameter space in the right panel of Fig. 3, where (m_h, m_l) are obtained after a numerical scan. We assume \tilde{m}_T to be in the range 5–10 TeV, where the latter coincides with the cutoff scale $4\pi f$, for $\xi = 0.1$. Moreover, we scan $1.5 \leq |r| \leq 5$, while the doublet masses are independently scanned in the range $2 \leq |m_{v,w}/m_s| \leq 4$. To obtain the correct top mass, we consider $1 \leq |y_{L,R}| \leq 2$. As we can see, the lightest fermion state can now be pushed above 3.5 TeV in the blue band corresponding to $100 \text{ GeV} \lesssim m_h \lesssim 125 \text{ GeV}$.

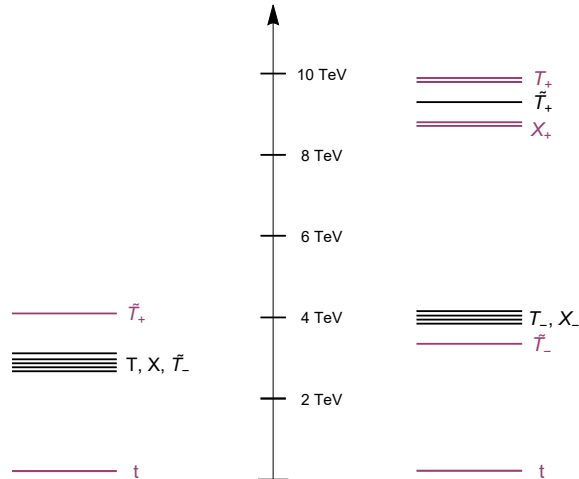


Figure 4. **Left:** The spectrum as resulting from the benchmark point B_s . The lightest particle mainly overlaps with the composite singlet \tilde{T} , with a mass $m_l \simeq 2.7$ TeV. The heaviest state mainly comes from the elementary singlet s with a mass ~ 4 TeV. The states colored by black are mainly composites, whereas the purple ones are mainly elementary. We have denoted by X the doublet other than T , forming the $SO(4)$ fourplet Q . **Right:** The spectrum as resulting from the benchmark point B_f . The lightest particle is mainly the elementary singlet s , with a mass $m_l \simeq 3.4$ TeV. We have denoted by X_{\pm} the eigenstates resulting from the mixing of X and w . Compared to the left panel, the effect of bringing down the doublets T_+ and X_+ is to lift the lightest state together with the composite resonances, which are found at 9.3 TeV (singlet of $SO(4)$) and at 4 TeV (fourplet of $SO(4)$).

4 Benchmark points

We now choose two benchmark points to show how the spectrum looks like, in the case in which only the elementary singlet vector-like fermion s is below the cut-off, presented at the beginning of Sec. 3.1, and in the case of Sec. 3.2 where all the elementary states are active.

For the singlet case we take B_s as

$$B_s : \{y_L = 1.4, y_R = 1.3, \tilde{m}_T = 3 \text{ TeV}, m_s = 3.8 \text{ TeV}\}, \quad (4.1)$$

so that $r = \tilde{m}_T/m_s \simeq 0.8$, $q = -0.9$ and $m_t \simeq 140$ GeV. Notice that $q^2 r^4 \simeq 0.3$, which is far from the (approximate) zero of β at $q^2 r^4 = 1$. The lightest eigenstate is the mainly composite singlet state \tilde{T}_- , with a mass $m_l \simeq 2.7$ TeV. The Higgs mass is found to be $m_h \simeq 110$ GeV. The spectrum is shown in the left panel of Fig. 4. The states coloured black correspond to mainly composite states, whereas the purple ones are mostly elementary. The composite resonances lie in the range 2.7 – 3.0 TeV. The heaviest state is the mainly elementary singlet \tilde{T}_+ with a mass around 4 TeV.

For the case discussed in Sec. 3.2, where all the elementary vector-like fermions

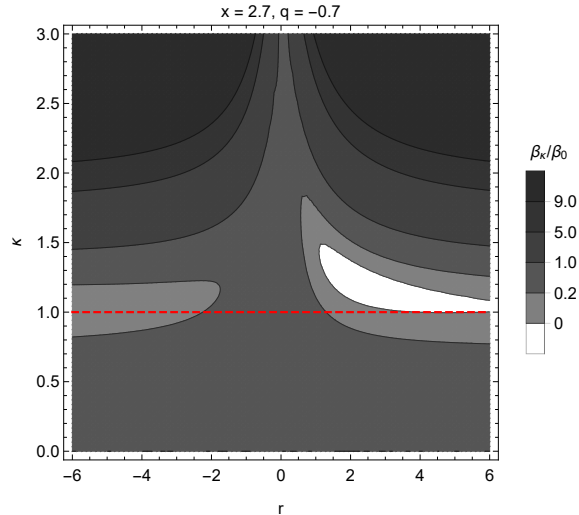


Figure 5. The ratio β_κ/β_0 as a contour plot in the (r, κ) plane for $x = 2.7$ and $q = -0.7$. The plot is mirrored for $\kappa \rightarrow -\kappa$. See text for details.

are kept in the spectrum, we take B_f to be

$$B_f : \{y_L = 1.8, y_R = 1.8, x = 2.8, y = 2.5, \tilde{m}_T = 9 \text{ TeV}, m_s = 3.5 \text{ TeV}\}, \quad (4.2)$$

which yields $q \simeq -0.4$ and $m_t \simeq 140 \text{ GeV}$. The lightest state is now the mostly elementary singlet \tilde{T}_- with $m_l \simeq 3.4 \text{ TeV}$. The Higgs mass is $m_h \simeq 120 \text{ GeV}$. The spectrum is given in the right panel of Fig. 4, where the same color convention is used to distinguish the mostly elementary states from the mainly composites. The overall effect of bringing the doublets v and w down with respect to left panel (where they are decoupled) is to lift the lightest state, which is now mostly elementary. This opens the possibility of having the spin-1/2 resonances of the strong dynamics closer to the cutoff $\Lambda \simeq 10 \text{ TeV}$, in this example $m_{\tilde{T}_+} \simeq 9.3 \text{ TeV}$ and $m_{T_-, X_-} \simeq 4 \text{ TeV}$.

5 The general case of vector-like elementary fermions

The setup discussed in Sec. 2 is based on the fact that the new vector-like fermions are embedded together with the chiral fermions to form complete $SO(5)$ representations. Therefore, partial compositeness now preserves the global symmetry and its breaking is sequestered to non-zero masses for the vector-like fermions.

We now relax this assumption and show what happens if the new fermions can couple arbitrarily to the composite resonances. To do so, we recompute β perturbing the partial compositeness couplings of s , v and w by a common factor κ (now referred to as β_κ), such that $\kappa = 0$ reproduces the MCHM₅ and $\kappa = 1$ corresponds to the analysis of Sec. 3.2 for the sMCHM₅.

The ratio β_κ/β_0 measures the degree of Goldstone breaking and is shown via a contour plot in Fig. 5, where $r = \tilde{m}_T/m_s$, $x = m_d/m_s = 2.7$, with m_d the degenerate mass of the doublets v and w , for a reference value of $q = m_Q/\tilde{m}_T = -0.7$. As we can see, increasing κ from zero helps reducing the Goldstone symmetry breaking, up to the point $\kappa \gtrsim 2$, from which on it is enhanced. The optimal region is indeed around $\kappa^2 \approx 1$, namely the $SO(5)$ symmetric point for partial compositeness. Thus, organizing the new elementary fermions to achieve complete $SO(5)$ representations (when possible) is not only motivated by symmetry arguments (see also the discussion on the holographic picture in Sec. 2) but it turns out to be in general the safest option to avoid light partners.

6 Conclusions

We have proposed a new way of breaking the Goldstone symmetry in CH scenarios, which is responsible for a non-vanishing Higgs potential. Instead of violating it via assuming the (SM-like) fermions not to fill complete representations of the global symmetry ($SO(5)$ in our case), we break it 'softly', i.e. via finite vector-like masses lifting the additional degrees of freedom that fill the representations beyond direct LHC reach (opposed to fully eliminating them from the spectrum). As we have shown explicitly for a two-side incarnation, this allows to reduce the amount of Goldstone-symmetry breaking such that the large top mass can be reproduced (for fixed f) without the necessity of vastly lowering the masses of the lightest top partners, the latter option starting to be in tension with LHC searches. For example, for $f \simeq 780$ GeV it is possible to lift the lightest partners from $m_l \lesssim 1$ TeV up to $m_l \sim 4$ TeV, coming closer to the general scale of CH resonances. While the light top partners might thus be hard to detect directly at the LHC (and are generically above current LHC limits), for this setup they would be fully discoverable at the FCC. In this context, we finally note that a further phenomenological survey of the proposed sMCHM would be interesting, including an analysis of electroweak precision observables, Higgs physics, and direct searches for (elementary and composite) fermionic resonances, which is however beyond the scope of the present article.

Acknowledgments

We are grateful to Roberto Contino and Tommi Alanne for useful discussions.

References

- [1] David B. Kaplan and Howard Georgi. $SU(2) \times U(1)$ Breaking by Vacuum Misalignment. *Phys. Lett.*, 136B:183–186, 1984.

- [2] David B. Kaplan, Howard Georgi, and Savas Dimopoulos. Composite Higgs Scalars. *Phys. Lett.*, 136B:187–190, 1984.
- [3] Michael J. Dugan, Howard Georgi, and David B. Kaplan. Anatomy of a Composite Higgs Model. *Nucl. Phys.*, B254:299–326, 1985.
- [4] David B. Kaplan. Flavor at SSC energies: A New mechanism for dynamically generated fermion masses. *Nucl. Phys.*, B365:259–278, 1991.
- [5] Kaustubh Agashe, Roberto Contino, and Alex Pomarol. The Minimal composite Higgs model. *Nucl. Phys.*, B719:165–187, 2005.
- [6] Roberto Contino, Yasunori Nomura, and Alex Pomarol. Higgs as a holographic pseudo-Goldstone boson. *Nucl. Phys.*, B671:148–174, 2003.
- [7] Roberto Contino, Leandro Da Rold, and Alex Pomarol. Light custodians in natural composite Higgs models. *Phys. Rev.*, D75:055014, 2007.
- [8] Oleksii Matsedonskyi, Giuliano Panico, and Andrea Wulzer. Light Top Partners for a Light Composite Higgs. *JHEP*, 01:164, 2013.
- [9] Alex Pomarol and Francesco Riva. The Composite Higgs and Light Resonance Connection. *JHEP*, 08:135, 2012.
- [10] Csaba Csaki, Adam Falkowski, and Andreas Weiler. The Flavor of the Composite Pseudo-Goldstone Higgs. *JHEP*, 09:008, 2008.
- [11] Stefania De Curtis, Michele Redi, and Andrea Tesi. The 4D Composite Higgs. *JHEP*, 04:042, 2012.
- [12] Florian Goertz. Composite Higgs theory. *PoS*, ALPS2018:012, 2018.
- [13] Adrian Carmona and Florian Goertz. A naturally light Higgs without light Top Partners. *JHEP*, 05:002, 2015.
- [14] Adrian Carmona and Florian Goertz. Lepton Flavor and Nonuniversality from Minimal Composite Higgs Setups. *Phys. Rev. Lett.*, 116(25):251801, 2016.
- [15] Adrian Carmona and Florian Goertz. A flavor-safe composite explanation of R_K . *Nucl. Part. Phys. Proc.*, 285-286:93–98, 2017.
- [16] Adrián Carmona and Florian Goertz. Recent \mathbf{B} Physics Anomalies - a First Hint for Compositeness? 2017.
- [17] Giuliano Panico, Michele Redi, Andrea Tesi, and Andrea Wulzer. On the Tuning and the Mass of the Composite Higgs. *JHEP*, 03:051, 2013.
- [18] Giuliano Panico and Andrea Wulzer. The Discrete Composite Higgs Model. *JHEP*, 09:135, 2011.